Research paper

Acta Neurobiol Exp 2017, 77: 57–67

ACTA NEUROBIOLOGIÆ EXPERIMENTALIS

Nicorandil attenuates neuronal mitochondrial dysfunction and oxidative stress associated with murine model of vascular calcification

Sriram Ravindran[1], Krithika Swaminathan[2], Abhinaya Ramesh[2], and Gino A. Kurian[1]*

*[1] Vascular Biology Lab, SASTRA University, Thanjavur, India, [2] School of Chemical and Biotechnology, SASTRA University, Thanjavur, India, * Email: kurian@scbt.sastra.edu*

Evidences suggest that the presence of chronic kidney disease (CKD) is associated with cerebrovascular diseases related cognitive decline in dialysis patients. As mitochondrial dysfunction is implicated in neurodegenerative disorders, we hypothesized that changes in brain mitochondria occur due to vascular calcification induced by renal failure and the opening of the mitochondrial potassium channel using nicorandil may prevent its dysfunction. Brain tissues from rats with vascular calcification were studied. Nicorandil (7.5 mg/kg b.wt.) was given either concomitantly or after the induction of calcification. The brain tissues were evaluated for antioxidant capacity, mitochondrial enzymes and oxidative phosphorylation efficiency along with the progression of calcification. The results suggested that renal failure, elevated the calcium, phosphorus product in the brain. The brain cytoplasm and mitochondrial fractions showed an elevated TBARS and a corresponding decline in the antioxidant enzymes, indicating a severe oxidative stress. The elevated brain mitochondrial enzymes like NADH dehydrogenase, and succinate dehydrogenase in the disease control groups, reversed to the near control level after nicorandil treatment. We observed that nicorandil was more effective when given after calcification. It reduced the biochemical alterations associated with calcium and phosphorous toxicity in the brain, by preserving mitochondria, the key target for treating neurodegenerative diseases.

Key words: brain mitochondria, nicorandil, adenine, vascular calcification, oxidative stress, calcium, phosphorous

INTRODUCTION

Chronic kidney disease (CKD) is a progressive loss of kidney function over a long time and is a very common clinical problem in elderly patients, associated with increased morbidity and mortality. Complications arising out of CKD include anemia, cardiovascular risk, dyslipidemia, mineral and bone disorder. Recently, Drew and Weiner (2014) have reported cognitive impairment in people with CKD, which support the findings of Vogels and others (2012) that CKD is associated with brain lesions, and are predictors of stroke, dementia and cognitive decline. These crebro-renal interactions are due to circulating uremic toxins such as uric acid, indoxyl sulfate, p-cresyl sulfate, interleukin 1-β, interleukin 6, TNF-α, and PTH has been reported by Watanabe and colleagues (2014). Calcium and phosphorous levels in blood and tissue also fall under this category, which is considered to be one of the key players of vascular calcification observed in patients with renal failure (Patsalas et al. 2007). However, much work has not been progressed in this aspect that leads to the limited understanding of the chemistry behind remote organ failure in the brain due to CKD and the role of its associated elevation in calcium and phosphorous to determine the magnitude of pathology.

Nicorandil, a clinically proven anti-angina agent (Goldschmidt et al. 1996), which acts as a nitric oxide donor, an antioxidant and ATP dependent K^+ channel activator is effective against acute renal failure as well (Tamura et al. 2012). It improves mitochondrial function through its activation of mitoK_{ATP} channels, preventing calcium overload and preserving membrane integrity (Nakae et al. 2000). Apart from the proven efficacy in treating CKD, nicorandil is also beneficial in patients with end stage renal disorders (ESRD) undergoing hemodialysis, by reducing oxidative damage (Ishii et al. 2007).

In the present study, we have evaluated the toxic outcome of adenine induced renal failure on the metabolic alterations in the rat brain and its mitochondria. Adenine is metabolized to form 8-hydroxy adenine as an insoluble end product which deposits in the kidney, leading to its damage and resulting in an increased circulating calcium and phosphorous levels along with the free

Received 30 September 2016, accepted 11 February 2017

Correspondence should be addressed to G.A. Kurian
Email: kurian@scbt.sastra.edu

radical outburst. Previous studies by Subhash and others (2015) showed that metabolic alteration due to adenine induced vascular calcification promotes mitochondrial free radical production that culminate in its dysfunction. Renal involvement in the mitochondrial cytopathies in the brain is an established concept. Hence, by using nicorandil, a mitoK_{ATP} channel opener, we evaluated its impact on brain mitochondrial bioenergetics, as a step towards improving cognitive impairment.

METHODS

Animals

All the experimental procedures were performed in accordance with the guidelines of the committee for the purpose of conduct and supervision of experiments on animals, Government of India and theinstitutional animal ethics committee of SASTRA University, Thanjavur (IAEC No. 258/SASTRA/IAEC/RPP). Eight weeks old male Wistar rats from the central animal facility at SASTRA University were maintained under controlled conditions at the 12-h day/night regime, water and food *ad libitum* for the study.

Chronic kidney disease model

The rats were acclimatized for 7 days and randomly assigned into 4 groups of 6 rats each as per the following schedule. Group 1-control: fed on normal rat chow, group2-induced: fed on rat chow mixed with 0.75% w/w adenine for 28 days, group 3-nicorandil preventive (Nic_pre): fed on the same diet as group 2 and administered nicorandil (7.5 mg/kg b.wt.) orally for 28 days concurrently, group 4: nicorandil curative (Nic_cur): similar to group 3 except that the administration ofnicorandilwas for 21 days after induction. At the end of the study, rats were euthanized and the brains were harvested for further assays.

Kidney function tests

Whole Blood was collected at the end of the study via retro orbital sinus under halothane anesthesia in K_2EDTA tubes and centrifuged for 5 min for plasma separation. Urine was collected and volume measured by placing the rats in metabolic cages 24 h prior to the day of euthanasia. The samples were stored at –80°C prior to analysis. Markers for acute and chronic kidney damage such as ALP, creatinine, urea and uric acidwere assessed using kits from Span diagnostics Ltd., India. Plasma protein was analyzed using a Bradford assay kit from Bio-Rad, CA, USA.

Calcium and phosphate analysis

Tissue samples mainly aorta and brain were processed for estimation of calcium and phosphorous. Briefly, organs were weighed and soaked in 0.5 N HCl for 24 h, followed by neutralization with 3 M NaOH. The supernatant was used for measuring the calcium and phosphorous level in these organs as an indicator of the mineralization processdue to kidney damage induced by adenine, as per kit instructions from Span diagnostics Ltd., India. Calcium estimation was based on formation of blue-purple colored complex using arsenazo III dye, which was measured at 650 nm. Phosphorous was estimated based on formation of phospho-molybdate complex, which was measured at 340 nm. All the spectrophotometric estimations were acquired using SYNERGY H1 multimode reader from BioTek U.S.A. The results were expressed as Ca×P product for comparison across the groups, as they exist as complex salts in the system rather than individual ions.

Tissue homogenization & mitochondria isolation

Brain tissues was homogenized using a Potter Elvehjem homogenizer (Remi-India) in ice cold isolation medium (250 mM sucrose, 1 mM EGTA, 10 mM HEPES; pH 7.4) supplemented with 0.5% bovine serum albumin (fatty acid free) and centrifuged at 1000× g for 5 min at 4°C. The supernatant was collected for assay of lipid peroxidation and antioxidant enzymes.

Crude Mitochondria were isolated from the brain as per previously described method of Lai and Clark (1979), with slight modification using sucrose based medium (250 mM sucrose, 1 mM EGTA, 10 mM HEPES; pH 7.4), by differential centrifugation. The centrifugation process separates the cell organelle based on their densities. After pelleting the nuclear fraction in the previous step, the supernatant was centrifuged at 2000× g for 3 min at 4°C to collect the supernatant containing crude mitochondria. This is followed by centrifugation at 14,000× g for 8 min at 4°C to pellet the crude mitochondria. The pellet was suspended in isolation buffer and stored at 4°C. Further assays were carried out after protein estimation using a Bradford assay kit from Bio-Rad, CA, USA.

Mitochondrial function and enzyme status

Mitochondrial respiration was monitored in the presence of glutamate/malate as substrate using Clarke type oxygen electrode from Hansatek, U.K. The respiratory control ratio (RCR=state 3/state 4) and ADP to oxygen (P/O) consumption ratio were assessed to measure the membrane

integrity and proton flux as per the standard procedures by Barrientos and others (2009).

Ca^{2+}-induced mitochondrial swelling was used to assess the opening of the mitochondrial permeability transition pore according to Martens and colleagues (1986). The light scattering was monitored at 540 nm for 8 min.

Mitochondrial membrane potential was estimated using the uptake of the positively charged fluorescent dye, rhodamine 123 in compliance of Perry and others (2011). Mitochondrial pellets were separated by centrifugation and the concentration of dye was measured at an ex/em 549/574 nm. Membrane potentials in millivolts were calculated according to the Nernst equation.

Mitochondrial pellets were ruptured using freeze thaw cycles and the complex enzymes were estimated as per established procedures. NADH dehydrogenase activity was determined according to Shapiro and colleagues (1979). The oxidation of NADH was monitored using potassium ferricyanide as electron acceptor and the fluorescent intensity was read at 340/470 nm. Malate dehydrogenase activity was measured according to Mullinax and others (1982) using oxaloacetate as substrate and the NADH oxidation was monitored at 340 nm for 10 min. SDH activity was estimated according to the method of Slater and Bonner (1951), using succinate as substrate and the potassium ferricyanide reduction was monitored at 455 nm for 10 min

In-gel assessment of mitochondrial complex-I and complex-V activities

The mitochondrial in-gel enzymatic activities for complex-I and complex-V were assessed according to Wittig and others (2007) using clear native PAGE. Briefly, 400µg protein was suspended in sample buffer (50 mM NaCl, 50 mM imidazole-HCl, 2 mM 6-aminohexanoic acid and 1 mM EDTA, pH 7.0) with DDM and incubated in ice followed by centrifugation at 20,000× g for 20 min at 4°C. The supernatant was loaded on to 5–13% gradient acrylamide gel and run for 100 V for 1 h followed by 200 V for 4 h at 4°C using cathode (50 mM Tricine, 7.5 mM imidazole, 0.01% DDM, pH 7.0) and anode (25 mM imidazole-HCl, pH 7.0) buffers. Post run, the gel was stained for complex-I reaction mixture (5 mM Tris-HCl, NADH and 2.5 mg/mL NBT) for 10 min to obtain a clear purple band corresponding to the enzyme activity. Complex V activity was assessed by staining in the reaction mixture (35 mM Tris-HCl, 128 mM Glycine, $MgCl_2$, 0.2% $PbNO_3$, 8 mM ATP, pH 8.3) for 3 h until the formation of white lead phosphate band was visualized. The images were obtained using ChemiDoc XRS (BioRad, USA) and the band intensities were quantified using Quantity one software (BioRad, USA).

Free radical scavenging potential of isolated mitochondria

The isolated brain mitochondria were evaluated for their free radical scavenging potential against superoxide radical and nitric oxide (Kurian et al. 2009). Briefly, the superoxide radical scavenging was evaluated by the nitro blue tetrazolium reduction method, in a reaction mixture (67 mM phosphate buffer pH 7.8, 6 mM EDTA, 3 mg NaCN, 2 mM riboflavin, 50 mM NBT) with 50 µg of mitochondrial protein. The percentage inhibition of super oxide generation was calculated by comparing the absorbance values of the control group at 530 nm. Nitric oxide was generated using sodium nitroprusside (5 mM in PBS) and estimated using Greiss reagent. The ability of mitochondria to reduce nitric oxide production was estimated from the absorbance of the chromophore formed during the diazotization of nitrite with sulphanilamide and subsequent coupling with napthylethylenediamine at 546 nm and compared to the absorbance of control group.

Lipid peroxidation and antioxidant enzymes

Lipid peroxidation and antioxidant enzymes were assayed both in the brain homogenate as well as the mitochondrial fraction. For all the estimation procedures, 100 ug/mL of final protein concentration was used. All the spectrophotometric estimations were carried out on high throughput and read using SYNERGY H1 multimode reader from BioTek, U.S.A.

Lipid peroxidation was determined by measurement of malondialdehyde chromogen formation using thiobarbituric acid according to the procedure of Ohkawa and colleagues (1979). Briefly, 100µL of sample was added to 0.8% thiobarbituric acid+15% trichloroacetic acid adjusted to pH 3.5 and kept in water bath maintained at 95°C for 1 h. Later the reaction mixture was cooled; butanol-pyridine mixture (15:1) was added to extract the pink colored complex and the absorbance of organic layer was read at 532 nm.

Catalase (CAT) was estimated by the method of Goldblith and Proctor (1950), and the rate of decomposition of $KMnO_4$ was measured at 515 nm. Briefly, 0.01 N H_2O_2 in phosphate buffer (pH 6.8) was added to the sample and mixed with 5 mM acidified $KMnO_4$. The excess peroxide was estimated by reacting with permanganate and measured using spectrophotometer.

SOD activity was estimated by the method of Nandi and Chatterjee (1988) and the inhibition of autoxidation of pyrogallol was measured at 420 nm. Briefly, 50µL of sample was mixed with 45 mM Tris+1 mM EDTA buffer (pH 7.4) and 2.5 mM pyrogallol was added to initiate the reaction. The autoxidation of pyrogallol was monitored

kinetically for 10 min at an interval of every 1 min using spectrophotometer.

GPx activity was assayed by the method of Sedlák (1987), using Ellman's reagent and read at 412 nm. Protein sample of 50μL was added to a reaction mixture (10 mM NaN_3, 4 mM GSH, 2.5 mM H_2O_2 prepared in phosphate buffer pH 7.4) and incubated for 10 min at room temperature. The enzyme activity was stopped using 10% trichloroaceticacid and the unreacted GSH was estimated using 0.04% Ellman's reagent prepared in 1% sodium citrate by spectrophotometer.

Histopathology of aorta

Von-Kossa staining was done to evaluate calcium deposition in the aorta. Embedded sections were deparaffinised and hydrated in a graded alcohol, followed by immersion in 5% silver nitrate and exposed to UV-light for 30 min. This was followed by treatment with 2% sodium thiosulfate for 5min and counter stained with 2% acidified neutral red before taking images.

Statistical analysis

Statistical analysis was performed using Graph pad Prism software. The results were expressed as mean ±S.D. The differences between groups were analyzed for statistical significance by using Student's t-test. The differences among the experimental groups were analyzed using a one-way analysis of variance (ANOVA). $P<0.05$ was considered to be statistically significant.

RESULTS

Increased calcium and phosphorous in the brain, which is secondary to renal failure is reduced by nicorandil

Adenine administration to the rats for 28 days resulted in loss of body weight (37%) and polyuria (75%) compared to the control group (Figs 1A and 1B). Nicorandil given as a curative treatment prevented weight loss (23%) and

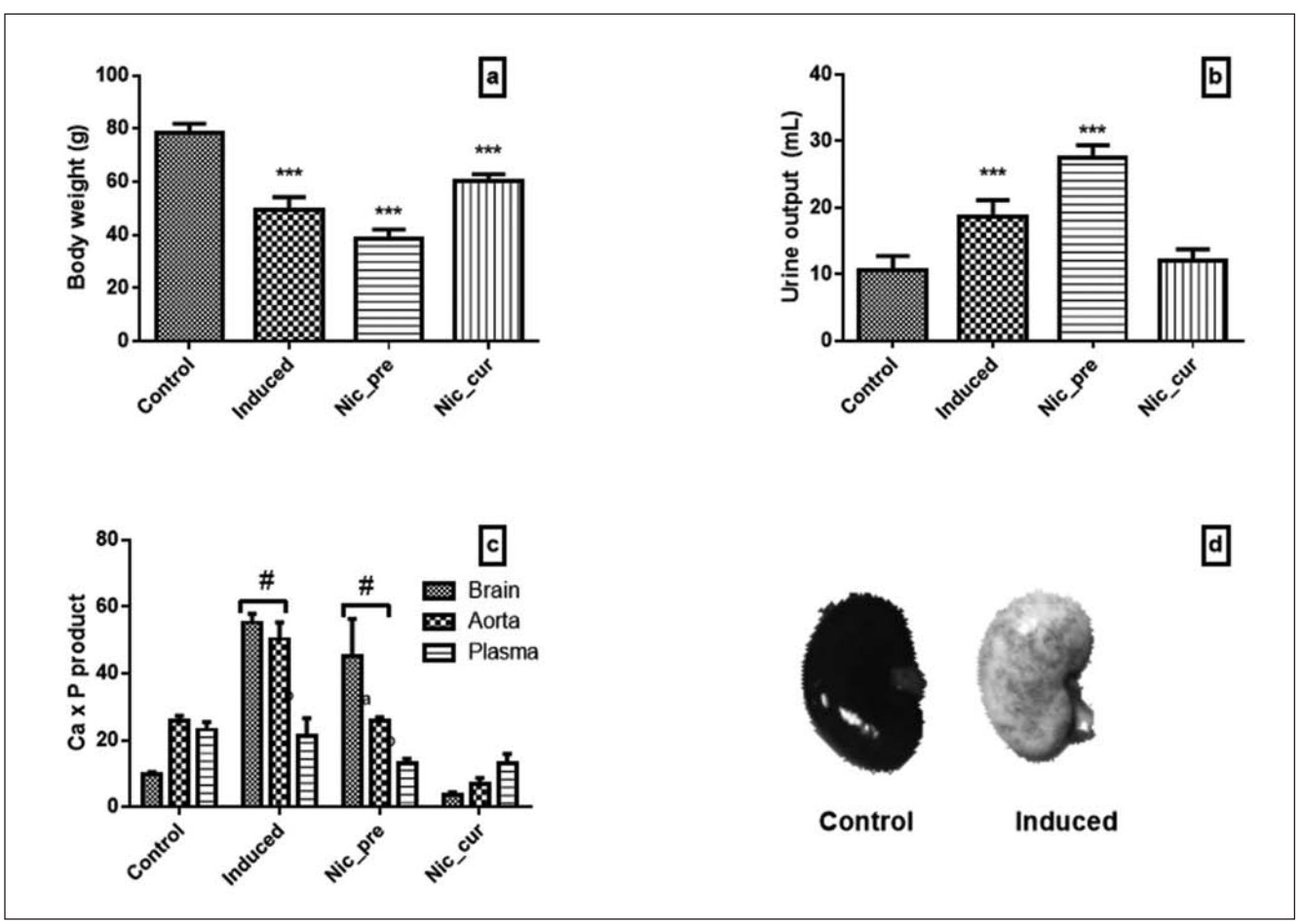

Fig. 1. Impact of adenine diet and treatment with nicorandil on (A) body weight, (B) urinary output, (C) Ca×P product and (D) kidney gross pathology of renal failure rats. Data expressed as mean ±S.D. (n=6), significant difference (***$P<0.001$, #, a, b $P<0.05$) *vs.* control, # *vs.* control Ca×P product, [a] brain *vs.* aorta, [b] brain *vs.* plasma.

restored urinary output (12%) compared to the control. This protective effect was not observed when nicorandil was administered as a preventive drug.

Plasma alkaline phosphatase (ALP), creatinine, urea and uric acidlevels are the primary indicators of renal damage and are reported to increase in such situations. Adenine treatment for 28 days significantlyincreased these parameters in plasma, 1.2 fold (ALP, $F_{3,13}$=145, P<0.001), 1.09 fold (creatinine, $F_{3,15}$=64, P<0.001), 3.96 fold (urea, $F_{3,13}$=389, P<0.001) and 13 fold (uric acid, $F_{3,8}$=181, P<0.001) as compared to the controlrats, indicating severe renal dysfunction (Table I). The estimated glomerular filtration rate (eGFR) dropped by 67% from the control level in adenine treated rats. Oral administration of nicorandil (7.5 mg/kg b.wt.) significantlyreduced the ALP ($F_{3,13}$=145, P<0.001), creatinine ($F_{3,15}$=64, P<0.001), urea ($F_{3,13}$=389, P<0.001) and uric acid ($F_{3,8}$=181, P<0.001) levels in plasma as compared with the induction control. Among the two nicorandil treated groups, Nic_cur showed superiorimprovement in renal function (Table I).

Hyperphosphatemia, a characteristic feature of adenine induced renal failure that results in the deposition of hydroxyapatite in various body compartments was prominent in adenine treated rats (Fig. 1C). We compared the levels of both calcium and phosphorous as their product in brain, aorta and plasma, as this model primarily induces calcification and stiffening of the aorta. The product was significantly ($F_{6,24}$=10, P<0.001) deposited in the brain (4.5 fold) and aorta (1.9 fold) of the induction group compared to the control rats (Fig. 1), however, its plasma levels remain constant across the groups. Treatment with nicorandil reduced Ca×P product significantly ($F_{6,24}$=10, P<0.001) in the brain (0.63 fold) and aorta (0.73 fold) of the Nic_cur group with no effect in Nic_pre, but its level in the aorta was near normalized compared to the control rats (Fig. 1C). In addition, we found a significant ($F_{6,24}$=10, P<0.001) decrease in the Ca×P product in plasma (0.44 fold) compared to the control, indicating a negative balance of the product by nicorandil. Furthermore, the gross pathology of the kidney (Fig. 1D) showed insoluble white depositions induced due to adenine administration, which confirmed the renal failure model. The histopathology of aortic rings showed reduction in mineral deposition, proving the effectiveness of nicorandil (Fig. 2D).

Effect of nicorandil on subcellular and cytosolic oxidative stress

Oxidative stress is usually measured by the extent of lipid peroxidation and activities of antioxidant enzymes in tissue as well as the sub cellular compartments. We evaluated the lipid peroxidation product (TBARS), the activity of superoxide dismutase (SOD), catalase and glutathione peroxidase (GPx) in both brain cytosolic and mitochondrial fraction separately to assess the compartmental stress variations due to calcium and phosphorous overload induced by renal failure (Fig. 3). TBARS content in the adenine induction group increased by 67% in cytosol and 96% in mitochondria, compared to the control (Fig. 3A). Nicorandil treatment significantly reduced TBARS (approx. 30%) in the cytosol compared to the induction group. On the contrary, brain mitochondrial TBARS was higher (89%, P<0.05) in Nic_pre groups, while Nic_curgroup showed a reduction (55%, P<0.05) in TBARS content compared to the control group.

The SOD activity in the induction group remained unchanged in the cytosol, while in mitochondria a reduction (65%) was observed compared to thecontrol, which was restored near normal by Nic_cur treatment (Fig. 2B). The decreased activity (P<0.05) of antioxidant enzymes after adenine treatment, as compared to the control in the cytosol (catalase – 45%, GPx – 53%) and mitochondria (catalase – 56%, GPx – 79%) were positively modified by nicorandil treatment (Figs 3C and 3D). Similar to the observation noted in lipid peroxidation, the activities of antioxidant enzymes (catalase and GPx) were restored to the near control value after nicorandil treatment, however the mitochondrial fraction still showed a persistently higher activity of these enzymes than in the cytosol (Figs 3C and 3D).

Table I. Kidney function tests in plasma showing ALP, creatinine, urea, uric acid and estimated GFR expressed as mean ±S.D. (n=6), significant difference (*P<0.05) *vs.* control

Group	Plasma				eGFR=Cr_urine/ Cr_plasma
	ALP (U/mg protein)	Creatinine (mg/dL)	Urea (mg/dL)	Uric acid (mg/dL)	
Control	0.25±0.01	0.46±0.02	13.00±1.20	1.13±0.03	3.21±0.41
Induced	0.57±0.02*	0.92±0.02*	64.54±1.56*	16.17±0.08*	1.06±0.34*
Nic_pre	0.22±0.02	0.63±0.02*	39.77±1.55*	7.25±0.06*	2.10±0.54*
Nic_cur	0.23±0.01	0.50±0.03	25.33±1.92*	6.91±0.04*	3.30±0.93

Values are mean ±S.D. *P<0.05. Cr – creatinine, eGFR – estimated glomerular filtration rate.

Effect of nicorandil on the brain mitochondrial functional activities

The functional analysis of mitochondria was done by measuring the changes in physiology, morphology and enzyme activities. An important aspect to limit mitochondrial dysfunction is the preservation of membrane integrity which is monitored by Ca2+ induced swelling and membrane potential (ΔΨ). The membrane potential was declined after adenine treatment compared to the normal range of (80–120 mv), but was restored significantly ($F_{7,22}$=48, P<0.05), after nicorandil was given as a curative drug, and is in accordance with swelling activity (Figs 4A and 4B), which indicates the intactmitochondrial morphology and functional state of the permeability transition pore (PTP) that controls the entry of Ca^{+2} ions into the mitochondrial matrix. A reduced absorbance at 540 nm would indicate increased light transmittance and swelling of matrix due to functional PTP, which is observed to be preserved better when nicorandil is given as curative drug. Mitochondrial respiration capacity, an indicator of intact mitochondrial membrane with a coupling efficiency was measured by oxygraph. Brain mitochondria showed a decline in the RCR and P/O ratio by 43% ($F_{3,12}$=20, P<0.05) and 33% ($F_{3,13}$=8.8, P<0.05) respectively after adenine treatment. Nicorandil when given as a curative agent significantly recovered the mitochondrial respiration to nearcontrol level (Figs 4C and 4D).

Mitochondrial enzyme activities were analyzed and the results are presented in Fig. 5. A significant increase in NADH dehydrogenase (1.8 fold, $F_{3,13}$=131, P<0.01) and SDH (1.3 fold, $F_{3,15}$=25, P<0.01) were observed in the adenine induction group, while MDH activity showed a decline (0.63 fold, $F_{3,10}$=40, P<0.01) compared to the control. The in-gel activity assessment of brain mitochondrial

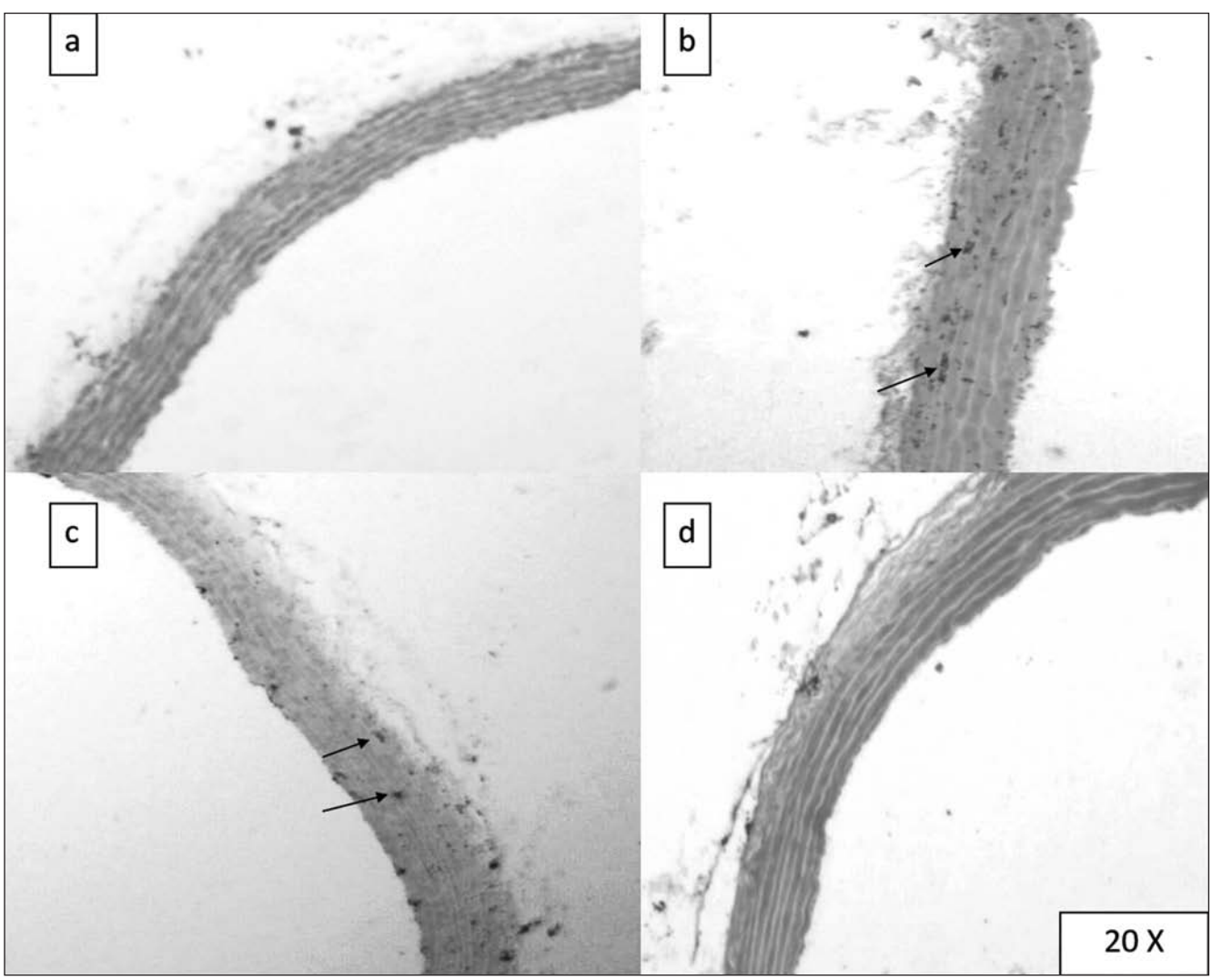

Fig. 2. Von-Kossa staining images of aorta sections (A) control (B) induced (C) Nic_pre and (D) Nic_cur, representing the calcium salts as black deposits indicated by arrow marks.

super-complex revealed an increased activity of complex-I (Fig. 5D) after adenine administration, while the complex-V activity declined (Fig. 5E) compared to the control brain. Nicorandil administered after the induction of renal failure restored the enzymes levels (NADH dehydrogenase, SDH and MDH) and in-gel complex-I activity to near normal, however the complex-V activity remained reduced by 40% (Fig. 5E), compared to the control.

The ability of isolated mitochondria to neutralize the free radicals depends on the activity of the scavenging enzymes within the organelle, which was measured indirectly based on its superoxide and nitric oxide scavenging potential. The ability of mitochondria to inhibit superoxide and nitric oxide formation was reduced by 31% and 22% respectively for superoxide and nitric oxide, after induction of renal impairment compared to the control. Nicorandil as a curative drug was able to restore its scavenging potential close to the control group (Table II).

Table II. Free radical scavenging capacity of isolated mitochondria against superoxide radical and nitric oxide expressed as mean ±S.D. (n=6), significant difference (*P<0.05) *vs.* control

Group	Superoxide (% inhibition of superoxide formation compared to control)	Nitric oxide (% inhibition of NO formation compared to control)
Control	100.00±3.4	100.00±3.6
Induced	69.42±4.1*	78.36±1.2*
Nic_pre	67.29±3.6*	77.01±5.9*
Nic_cur	98.32±2.9	95.80±6.2

Values are mean ±S.D. *P<0.05.

DISCUSSION

In this study, we demonstrated that renal tissue injury and its linked calcium, phosphorus product deposition in the aorta induced neuronal mitochondrial dysfunction, and the curative treatment with nicorandil prevented this

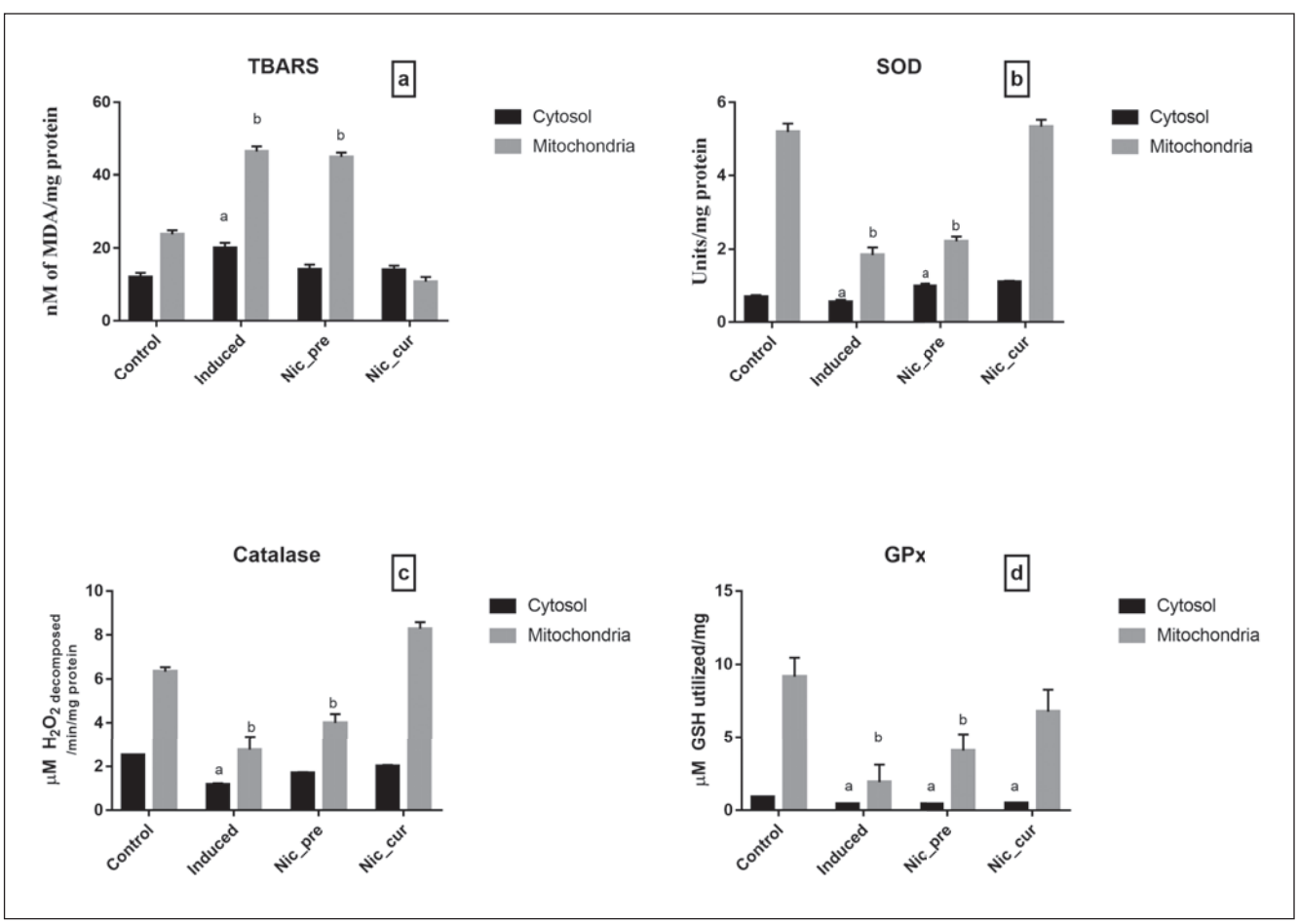

Fig. 3. Lipid peroxidation represented by the level of (A) thiobarbituric acid reactive species (TBARS) and the antioxidant enzyme status of (B) superoxide dismutase (SOD), (C) catalase and (D) glutathione peroxidase (GPx), in the cytosol and mitochondrial fractions of the rat brain fed on adenine diet and treated with nicorandil, expressed as mean ±S.D. (n=6). [a] significant difference (P<0.05) *vs.* cytosol control, [b] significant difference (P<0.05) *vs.* mitochondria control.

injury and associated brain mitochondrial dysfunction. Recent studies by Subhash and others (2015) have shown a direct link between the arterial calcification of major arteries and vascular brain disease where common link is believed to be mitochondrial K_{ATP} channel. Nicorandil, a selective mitochondrial K_{ATP} channel opener (Tamura et al. 2012) is understood to have dual actions, a nitrate-like action (Yang et al. 2005) and an action on K_{ATP} channels (Nakae et al. 2000). ATP-sensitive K^+ channels in the brain directly couple the cellular energy metabolism to electrical activity and play multifactorial roles in protecting against brain injury following hypoxia, ischemia or metabolic inhibition. Mitochondrial K_{ATP} activity as measured by rhodamine 123 assays and reconfirmed by osmotic swelling, in the isolated rat brain mitochondria, showed significant improvement with nicorandil administration especially when the treatment was given after the induction of calcification. Activating mitoK_{ATP} channel by nicorandil can increase the uptake of potassium in the mitochondrial matrix which could maintain mitochondrial matrix volume by attenuating Ca^{2+} loading (Rousou et al. 2004). Furthermore, nicorandil is believed to activate cytoplasmic guanylate cyclase leading to an increase in cellular levels of cGMP with a reduction in cytosol calcium and thereby reducing the Ca×P product load and its subsequent deposition (Shono et al. 1997). This was evident from restoration of the kidney function and reduction in calcium deposition in the aortic sections as observed from the histopathology.

Calcification was previously considered to be a passive process, now believed to be an actively regulated process where vascular cells are transformed to osteoblast like cells. Mitochondria play significant role in this process where insoluble calcium phosphate salts are deposited in the mitochondrial matrix (Millane et al. 1994). Mitochondrial dysfunction is the common pathological features in the diseases related to calcification (Ahn et al. 2010). Hence, mitochondrial physiology, morphology and enzyme activity measurement can be a promising marker to assess the pathology linked with calcification.

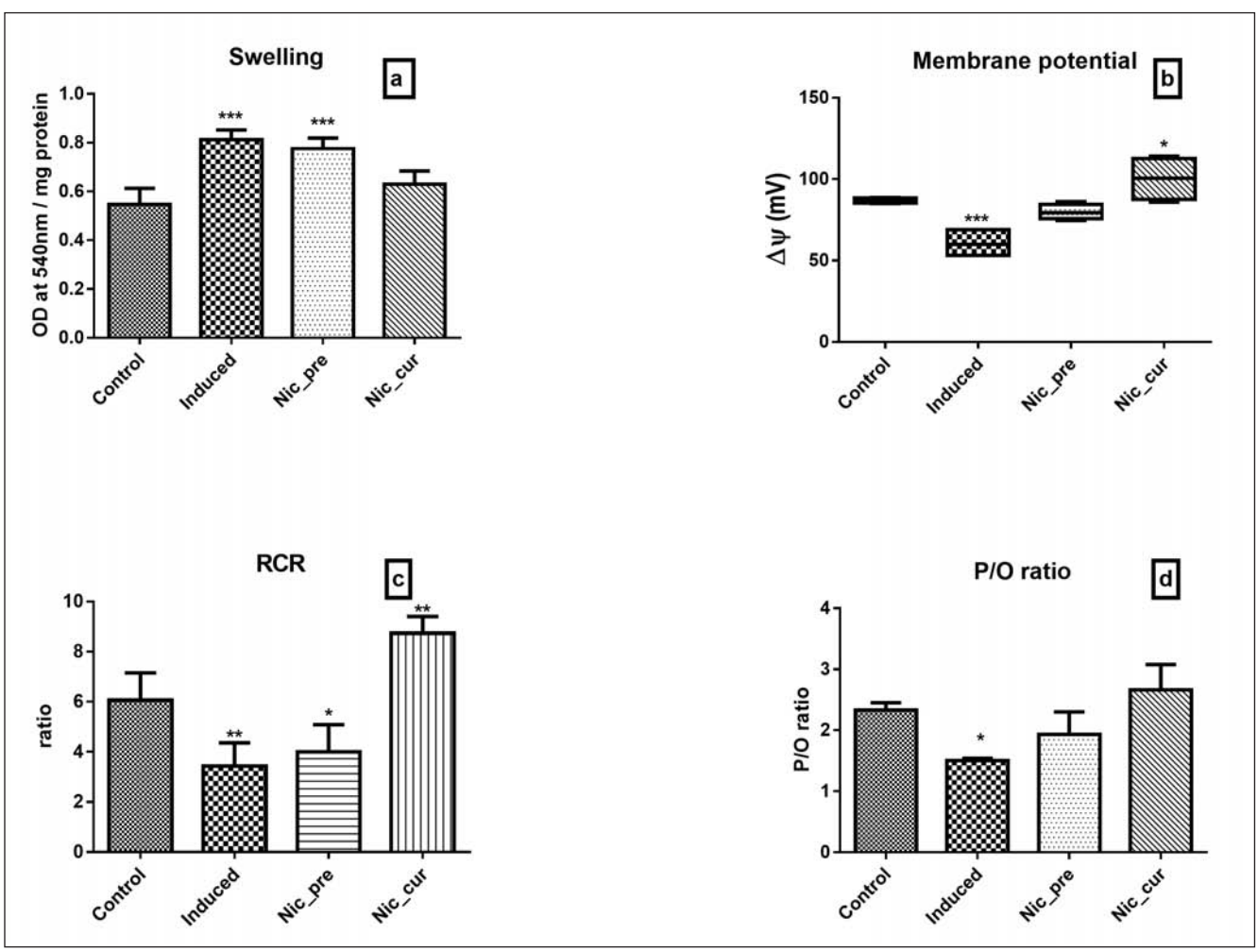

Fig. 4. Brain mitochondrial physiology expressed as (A) swelling, (B) membrane potential (C) RCR and (D) P/O ratio. Data expressed as mean ±S.D. (n=6), significant difference (*P<0.05, **P<0.01, ***P<0.001) *vs.* control.

In this context, we assessed the mitochondrial physiology (P/O, RCR), morphology (MPTP and swelling behavior), enzyme activities (MDH, SDH, NADH dehydrogenase) and in-gel super complex activity (complex I and V) in different experimental groups. Prominent mitochondrial dysfunction shown by the adenine treated animals was recovered significantly by nicorandil treatment. Modulation of mitoK_{ATP} by nicorandil may regulates the mitochondrial matrix volume and preserve the architecture of the intermembrane space, slowing ATP hydrolysis and preserving the ability to use creatine efficiently. However, in the present study, we found that nicorandil had better efficacy with the curative mode of treatment rather than preventive. This may be due to the ability of nicorandil to restore the altered mitochondria as shown by other investigators such as Carreira and colleagues (2008). Nicorandil reverses the negative effect of vascular calcification on brain mitochondria, by increasing the RCR (an indicator mitochondrial structural integrity) to the levels similar to those of control mitochondria (Fig. 4C) and increasing oxidative phosphorylation capacity compared to the controls (Fig. 4D), which is confirmed by the in-gel activity that measures the intact mitochondrial super complex ATP producing capacity (Figs 5D and 5E). Respiratory rate in state 4 indicates the index of proton leak and is mostly affected by uncoupling, which was found to be lower for the induced group treated with nicorandil and this effect was prominent in curative groups, indicates less uncoupling, which may reflect the greater integrity of the mitochondrial membrane for effective oxidation phosphorylation.

Another interesting observation, we made in our study is that brain mitochondrial dehydrogenase enzymes were elevated in the induction group animal, that indirectly enlighten the presence of calcium as previous studies showed that Ca^{2+} entry in the mitochondrial matrix activates the dependent mitochondrial dehydrogenase enzymes (Contreras and Satrustegui 2009). However, calcium mediated metabolic regulation also depends on the phosphate levels in mitochondria. It is believed that in brain mitochondria, calcium and phosphorus may combine to form amorphous $Ca_3(PO_4)_2$ and this complex dissociate into Ca^{2+} and Pi when the mitochondria are depolarized, so that Ca^{2+} exits via the reversal of the uniporter, and Pi exits via the Pi transporter. Nicorandil, by modulating the K_{ATP} channel, regulates the membrane potential (Fig. 4B) and thereby mediates the dissociation of amorphous $Ca_3(PO_4)_2$ in the matrix.

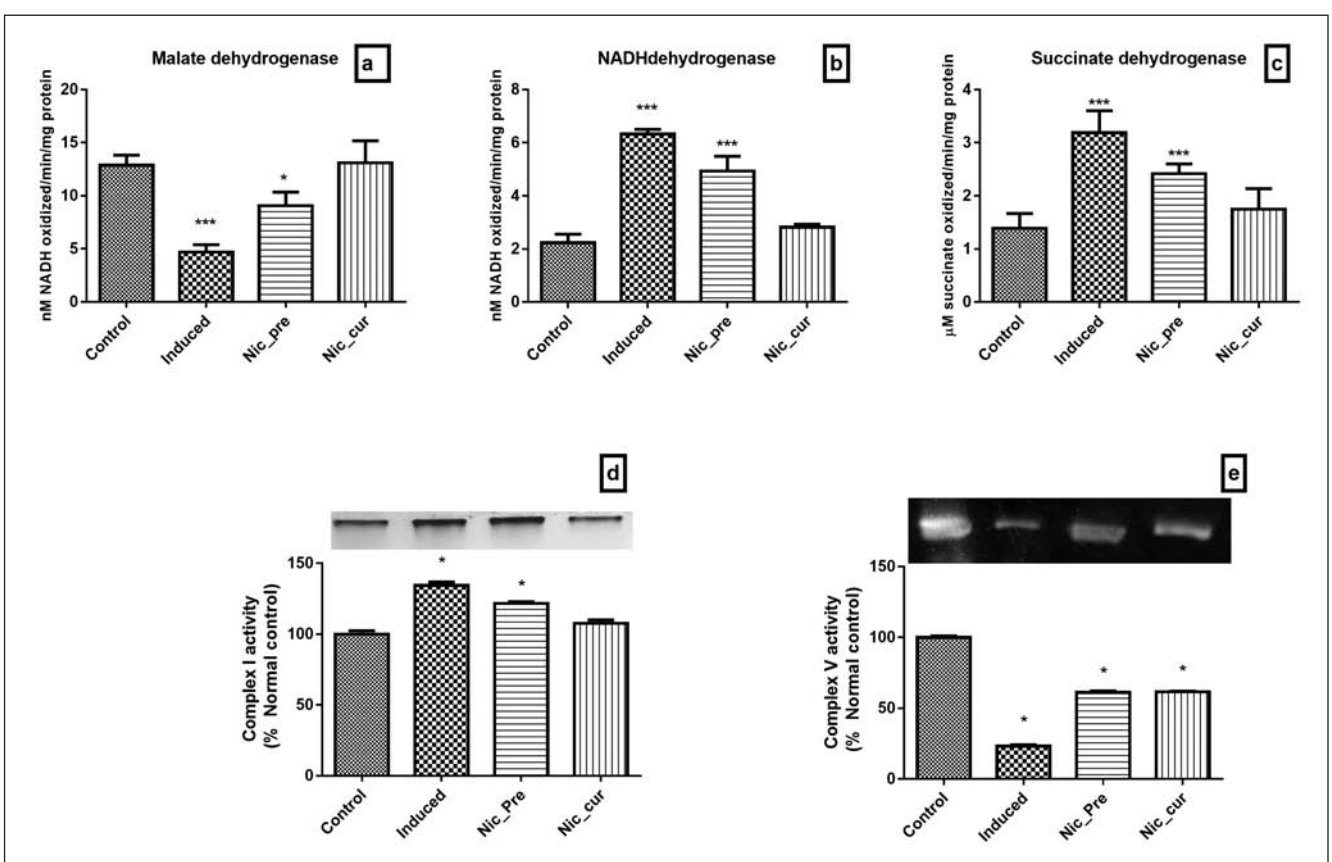

Fig. 5. Brain mitochondrial enzyme status represented by (A) NADH dehydrogenase, (B) succinate dehydrogenase and (C) malate dehydrogenase and in-gel activity assessment for (D) complex-I and (E) complex-V. Data expressed as mean ±S.D. (n=6), significant difference (*P<0.05, ***P<0.01) *vs.* control.

There are growing evidences that correlate the calcium overload and ROS release in the mitochondria that ultimately leads to the membrane permeability transition followed by cell death (Singh et al. 2011). In the present study, we observed that nicorandil significantly reversed the elevated levels of lipid peroxidation and decreased GSH level in the brain tissue ofadenine induced calcified animal. A corresponding increase in antioxidant enzymes, namely catalase, SOD and GPx underlines the efficacy of nicorandil in the reduction of oxidative stress, which was supported by the restoration of the radical scavenging ability of isolated mitochondrial fraction. Clinically available mitoK_{ATP} channel opener, nicorandil reported in the prevention of oxidative stress-induced apoptosis in neurons by preserving mitochondrial membrane potential (Teshima et al. 2003). Furthermore, Zhao and others (2011) provide a mechanistic link between the vascular calcification, increased mitochondrial membrane potential, increased mitochondrial reactive oxygen, followed by subsequent expression of osteogenic genes and vascular mineralization. This pathological nexus was de-linked by the nicorandil treatment. However, throughout the experiments we found that the curative mode of nicorandil treatment seems to be more beneficial and of therapeutic use. This observation underlines the significant therapeutic potential of nicorandil as a drug for the treatment of vascular calcification. The link between the ATP sensitive K_{ATP} channel and reactive oxygen species clarifies the intracellular mechanism of vascular calcification and may allow exploration of mitochondrial K_{ATP} channel modulator and antioxidants as therapeutic agents for vascular calcification.

CONCLUSION

In conclusion, we showed that nicorandil exerts its neuro-protective effect via preserving neuronal mitochondria and reducing oxidative stress in an adenine induced vascular calcification model. This finding demonstrates the therapeutic potential of nicorandil in treating mitochondrial dysfunction in brain implicated due to vascular calcification.

ACKNOWLEDGEMENTS

The project was supported by the TRR research grant awarded to Dr. Gino A. Kurian by SASTRA University, Thanjavur, India. The authors would like to acknowledge the Honorable Vice-Chancellor and the management of SASTRA University, Thanjavur, India for providing facilities to conduct animal experimentation.

REFERENCES

Ahn SY, Choi YS, Koo HJ, Jeong JH, Park WH, Kim M, Piao Y, Pak YK (2010) Mitochondrial dysfunction enhances the migration of vascular smooth muscles cells via suppression of Akt phosphorylation. Biochim Biophys Acta 1800(3): 275–281.

Barrientos A, Fontanesi F, Diaz F (2009) Evaluation of the mitochondrial respiratory chain and oxidative phosphorylation system using polarography and spectrophotometric enzyme assays. Curr Protoc Hum Genet. Chapter 19. Unit 19.3.

Carreira RS, Monteiro P, Kowaltowski AJ, Goncalves LM, Providencia LA (2008) Nicorandil protects cardiac mitochondria against permeability transition induced by ischemia-reperfusion. J Bioenerg Biomembr 40(2): 95–102.

Contreras L, Satrustegui J (2009) Calcium signaling in brain mitochondria: interplay of malate aspartate NADH shuttle and calcium uniporter/ mitochondrial dehydrogenase pathways. J Biol Chem 284(11): 7091–7099.

Drew DA, Weiner DE (2014) Cognitive impairment in chronic kidney disease: keep vascular disease in mind. Kidney Int 85(3): 505–507.

Goldblith SA, Proctor BE (1950) Photometric determination of catalase activity. J Biol Chem 187(2): 705–709.

Goldschmidt M, Landzberg BR, Frishman WH (1996) Nicorandil: a potassium channel opening drug for treatment of ischemic heart disease. J Clin Pharmacol 36(7): 559–572.

Ishii H, Toriyama T, Aoyama T, Takahashi H, Yamada S, Kasuga H, Ichimiya S, Kanashiro M, Mitsuhashi H, Maruyama S, Matsuo S, Naruse K, Matsubara T, Murohara T (2007) Efficacy of oral nicorandil in patients with end-stage renal disease: a retrospective chart review after coronary angioplasty in Japanese patients receiving hemodialysis. Clin Ther 29(1): 110–122.

Kurian GA, Rajamani T, Ramanarayanan P, Paddikkala J (2009) A comparative study on in vitro and in vivo antioxidant activities of aqueous extract of Desmodium gangeticum (Leguminosae) root. International Journal of Green Pharmacy 3(4): 8.

Lai JC, Clark JB (1979) Preparation of synaptic and nonsynaptic mitochondria from mammalian brain. Methods Enzymol 55: 51–60.

Martens ME, Chang CH, Lee CP (1986) Reye's syndrome: mitochondrial swelling and Ca2+ release induced by Reye's plasma, allantoin, and salicylate. Arch Biochem Biophys 244(2): 773–786.

Millane T, Wilson AJ, Patel MK, Jennison SH, Holt DW, Murday AJ, Camm AJ (1994) Mitochondrial calcium deposition in association with cyclosporine therapy and myocardial magnesium depletion: a serial histologic study in heart transplant recipients. J Heart Lung Transplant 13(3): 473–480.

Mullinax TR, Mock JN, McEvily AJ, Harrison JH (1982) Regulation of mitochondrial malate dehydrogenase. Evidence for an allosteric citrate-binding site. J Biol Chem 257(22): 13233–13239.

Nakae I, Takaoka A, Mitsunami K, Yabe T, Ito M, Masayuki, Takahashi, Matsumoto T, Omura T, Yokohama H, Kinoshita M (2000) Cardioprotective effects of nicorandil in rabbits anaesthetized with halothane: potentiation of ischaemic preconditioning via KATP channels. Clin Exp Pharmacol Physiol 27(10): 810–817.

Nandi A, Chatterjee IB (1988) Assay of superoxide dismutase activity in animal tissues. Journal of Biosciences 13(3): 305–315.

Ohkawa H, Ohishi N, Yagi K (1979) Assay for lipid peroxides in animal tissues by thiobarbituric acid reaction. Anal Biochem 95(2): 351–358.

Patsalas S, Eleftheriadis T, Spaia S, Theodoroglou H, Antoniadi G, Liakopoulos V, Passadakis P, Vayonas G, Vargemezis V (2007) Thirty-month follow-up of coronary artery calcification in hemodialysis patients: different roles for inflammation and abnormal calcium-phosphorous metabolism?. Ren Fail 29(5): 623–629.

Perry SW, Norman JP, Barbieri J, Brown EB, Gelbard HA (2011) Mitochondrial membrane potential probes and the proton gradient: a practical usage guide. Biotechniques 50(2): 98–115.

Rousou AJ, Ericsson M, Federman M, Levitsky S, McCully JD (2004) Opening of mitochondrial KATP channels enhances cardioprotection through the modulation of mitochondrial matrix volume, calcium accumulation, and respiration. Am J Physiol Heart Circ Physiol 287(5): H1967–H1976.

Sedlák J (1987) Effect of denervation on glutathione and oxidized glutathione in rat adrenal cortex and medulla after repeated stress. Endocrinol Exp 21(4): 263–268.

Shapiro BL, Feigal RJ, Lam LF (1979) Mitrochondrial NADH dehydrogenase in cystic fibrosis. Proc Natl Acad Sci U S A 76(6): 2979–2983.

Shono M, Houchi H, Oka M, Nakaya Y (1997) Effects of nitroprusside and nicorandil on catecholamine secretion and calcium mobilization in cultured bovine adrenal chromaffin cells. J Cardiovasc Pharmacol 30(4): 419–423.

Singh BK, Tripathi M, Pandey PK, Kakkar P (2011) Alteration in mitochondrial thiol enhances calcium ion dependent membrane permeability transition and dysfunction in vitro: a cross-talk between mtThiol, Ca(2+), and ROS. Mol Cell Biochem 357(1–2): 373–385.

Slater EC, Bonner WD (1951) Inhibition of the succinic oxidase system by fluoride. Biochem J 49(4): l–li.

Subhash N, Sriram R, Kurian GA (2015) Sodium thiosulfate protects brain in rat model of adenine induced vascular calcification. Neurochem Int 90: 193–203.

Tamura Y, Tanabe K, Kitagawa W, Uchida S, Schreiner GF, Johnson RJ, Nakagawa T (2012) Nicorandil, a $K_{(atp)}$ channel opener, alleviates chronic renal injury by targeting podocytes and macrophages. Am J Physiol Renal Physiol 303(3): F339–F349.

Teshima Y, Akao M, Baumgartner WA, Marban E (2003) Nicorandil prevents oxidative stress-induced apoptosis in neurons by activating mitochondrial ATP-sensitive potassium channels. Brain Res 990(1–2): 45–50.

Vogels SC, Emmelot-Vonk MH, Verhaar HJ, Koek HL (2012) The association of chronic kidney disease with brain lesions on MRI or CT: a systematic review. Maturitas 71(4): 331–336.

Watanabe K, Watanabe T, Nakayama M (2014) Cerebro-renal interactions: impact of uremic toxins on cognitive function. Neurotoxicology 44: 184–193.

Wittig I, Karas M, Schagger H (2007) High resolution clear native electrophoresis for in-gel functional assays and fluorescence studies of membrane protein complexes. Mol Cell Proteomics 6(7): 1215–1225.

Yang Q, Zhang RZ, Yim AP, He GW (2005) Release of nitric oxide and endothelium-derived hyperpolarizing factor (EDHF) in porcine coronary arteries exposed to hyperkalemia: effect of nicorandil. Ann Thorac Surg 79(6): 2065–2071.

Zhao MM, Xu MJ, Cai Y, Zhao G, Guan Y, Kong W, Tang C, Wang X (2011) Mitochondrial reactive oxygen species promote p65 nuclear translocation mediating high-phosphate-induced vascular calcification in vitro and in vivo. Kidney Int 79(10): 1071–1079.